Computational inverse holographic imaging: toward perfect reconstruction of wavefield distributions

Vladimir Katkovnik, Artem Migukin, Jaakko Astola
Signal Processing Institute, Tampere University of Technology,
P. O. Box 553, Tampere, Finland.
E-mails: {vladimir.katkov, artem.migukin, jaakko.astola}@tut.fi.

1 Introduction

Let $u_d(x,y)$ be a complex-valued 2D wavefield defined in the sensor plane $z=d$ as a function of the lateral coordinates x and y. According to the scalar diffraction theory there is a linear diffraction operator D_z linking the sensor wavefield distribution with the object wavefield $u_0(x,y)$ in the object plane $z=0$ as $u_d(x,y)=D_d\{u_0\}$. The inverse of this operator defines the estimate of u_0 from u_d as $\hat{u}_0(x,y)=D_{-d}\{u_d\}$. This estimate is perfect (precise for any u_0), $\hat{u}_0=u_0$, only provided that $u_d(x,y)$ is given for all (x,y), i.e. the sensor is of the infinite size [1].

Starting from the early days of the digital holography (70-80th of the 20th century) the algorithms developed and in conventional use for coherent imaging (at least in most planar optical setups) are based on digital approximations of the inverse operator D_{-z}. These algorithms can be given in the form $\hat{u}_0(x,y)=\hat{D}_{-z}\{u_z\}$, where the hat stands for a discrete approximation of D_{-z}. All of these discrete algorithms (convolutional methods, the Fourier and Fresnel transforms, etc.) inherit the principal limitation of the integral inverse operator D_{-z} and are not able to give a perfect reconstruction of the object wavefield just because of the finite size of the sensor.

Contrary to it the *inverse imaging* paradigm is based on a numerical inverse of the *forward* propagation operator D_z. The finite size of the sensor may result in the ill-conditioning of this inverse problem. This limitation being of a mathematical nature to some extend can be overcome or at least attenuated in the imaging using special computational methods.

The starting point of the inverse technique considered in this paper is a matrix digital approximation $\hat{D}_z$ of D_z for the finite size sensor output proposed in [2] and used for calculation and analysis of the forward and backward operators. This matrix model is precise and aliasing free for pixel-wise invariant object distributions exactly as it is for the frequency domain model developed in [3].

The results and discussion in this paper are focused on phase-object distributions. It is shown that the rank of the matrices in the matrix forward propagation model can be used as good indicators of the accuracy of the object distribution reconstruction. In this way this paper is an essential complement to [2], where all experiments concern amplitude-object distributions only.

2 Matrix Discrete Diffraction Transform (M-DDT)

Let the pixels in the object and sensor planes can be rectangular of the different sizes ($\Delta_{y,0} \times \Delta_{x,0}$) and ($\Delta_{y,z} \times \Delta_{x,z}$), respectively. Assuming the Fresnel approximation of the kernel in the diffraction operator D_z the discrete forward propagation model can be presented in the form [2]:

$$\mathbf{u}_z = \mu \cdot \mathbf{A}_y \cdot \mathbf{u}_o \cdot \mathbf{A}_x^T, \ \mu = -j \exp(j 2\pi \cdot z / \lambda) / (\lambda \cdot z) \qquad (1)$$

where $\mathbf{u}_z = (\mathbf{u}_z[s,t])_{N_{y,z} \times N_{x,z}}$ and $\mathbf{u}_0 = (\mathbf{u}_0[k,l])_{N_{y,0} \times N_{x,0}}$ are matrices of complex-valued wavefield distributions in the sensor and object planes, respectively. Elements of the "*averaged*" transfer matrices $\mathbf{A}_y = (\mathbf{A}_y[s,k])_{N_{y,z} \times N_{y,0}}$, $\mathbf{A}_x = (\mathbf{A}_x[t,l])_{N_{x,z} \times N_{x,0}}$ are calculated as

$$\mathbf{A}_y[s,k] = \frac{1}{\Delta_{y,z}} \int_{-\Delta_{y,z}/2}^{\Delta_{y,z}/2} \int_{-\Delta_{y,0}/2}^{\Delta_{y,0}/2} \exp[\frac{j\pi}{\lambda z}(k\Delta_{y,0} - s\Delta_{y,z} + \xi + \xi')^2] d\xi d\xi' \qquad (2)$$

$$\mathbf{A}_x[t,l] = \frac{1}{\Delta_{x,z}} \int_{-\Delta_{x,z}/2}^{\Delta_{x,z}/2} \int_{-\Delta_{x,0}/2}^{\Delta_{x,0}/2} \exp[\frac{j\pi}{\lambda z}(l\Delta_{x,0} - t\Delta_{x,z} + \eta + \eta')^2] d\eta d\eta' \qquad (3)$$

The matrices $\mathbf{A}_y$ and $\mathbf{A}_x$ manipulate by rows and columns of the object matrix $\mathbf{u}_0$, respectively. The formula (1) defines what we call *Matrix Discrete Diffraction Transform* (*M-DDT*). It is shown in [2] that calculations of the double integrals in Eq. (2) and (3) can be reduced to integration on single variables. By definition, the *M-DDT* defines the propagation model which is precise for any pixel-wise invariant (pixelated) object distribution. Being precise, this is an aliasing free model.

3 Inverse reconstruction of object distribution

When the accurate discrete forward propagation model is built, then, in principal, the accurate reconstruction of the object distribution $\mathbf{u}_0$ from $\mathbf{u}_z$ is possible. Formally, it can be done as a solution of Eq. (1). This solution gives the inverse of the forward propagation and defines what can be called *inverse backward propagation modeling*. If the accurate inverse can be found the perfect reconstruction of the pixelated object distribution can be achieved. Thus, due to the proposed matrix model the problems of the perfect reconstruction are reduced to the corresponding algebraic ones.

For rectangular object and sensor planes the perfect reconstruction can be achieved provided the following assumptions:

1. The support of the sensor plane distribution is equal or larger than the support of the object plane distribution ($N_{x,z} \geq N_{x,0}$ and $N_{y,z} \geq N_{y,0}$);
2. The $\mathbf{A}_y$ and $\mathbf{A}_x$ are full rank matrices, $rank(\mathbf{A}_y) = N_{y,0}$, $rank(\mathbf{A}_x) = N_{x,0}$.

If the conditions 1 and 2 are satisfied then the perfect reconstruction $\hat{\mathbf{u}}_0 = \mathbf{u}_0$ is given with the following formula:

$$\hat{\mathbf{u}}_o = (1/\mu) \cdot (\mathbf{A}_y^H \mathbf{A}_y)^{-1} \mathbf{A}_y^H \mathbf{u}_z \mathbf{A}_x^* (\mathbf{A}_x^T \mathbf{A}_x^*)^{-1} \tag{4}$$

where $(\cdot^{\mathrm{H}})$ stands for the Hermitian conjugate, $\mathbf{A}_y^H = (\mathbf{A}_y^*)^T$.

The numerical study shows that depending on the parameters, in particular, on the distance *d*, pixel's sizes, and object and sensor sizes the matrices $\mathbf{A}_y^H \mathbf{A}_y$ and $\mathbf{A}_x^H \mathbf{A}_x$ can be extremely ill-conditioned. This ill-conditioning means that these matrices are *numerically singular* and the formula (4) being formally correct practically is useless. The corresponding calculations cannot be fulfilled and gives unstable results highly sensitive with respect to the parameter variations, round off errors of calculations and observation noise. The regularization, for instance the standard Tikhonov`s one, is a conventional technique for various ill-conditioned problems. Instead of the solution (4) we are looking for the regularized estimate of $\mathbf{u}_0$ defined by minimization of the quadratic criterion:

$$\hat{\mathbf{u}}_0 = \arg\min_{\mathbf{u}_0}\{L\},\ L = \| \mathbf{u}_z - \mu \cdot \mathbf{A}_y \cdot \mathbf{u}_0 \cdot \mathbf{A}_x^T \|_F^2 + \alpha \| \mathbf{u}_0 \|_F^2 \tag{5}$$

where the Frobenius norm $\| \mathbf{u}_0 \|_F^2$ is the Tikhonov`s regularization penalty. The regularization parameter $\alpha \geq 0$ controls the level of

regularization or smoothness of $\hat{\mathbf{u}}_0$. It is shown in [2] that this regularized inverse can be given in the form

$$\hat{\mathbf{u}}_0 = (1/\mu)\cdot(\mathbf{A}_y^H\mathbf{A}_y + (\alpha/\mu)\mathbf{I})^{-1}\mathbf{A}_y^H\mathbf{u}_z\mathbf{A}_x^*(\mathbf{A}_x^T\mathbf{A}_x^* + (\alpha/\mu)\mathbf{I})^{-1} \quad (6)$$

The inverse wavefield reconstruction is a general and flexible approach applicable for different optical setups. However, we wish to emphasize that practically the accuracy of the reconstruction (6) depends seriously on the rank of the matrices $\mathbf{A}_y^H\mathbf{A}_y$ and $\mathbf{A}_x^H\mathbf{A}_x$ as it is illustrated in [2] and in the next section. It is confirmed by multiple simulation experiments that the rank of these matrices give a clear indication of the accuracy of reconstruction.

4 Simulations

We consider the discrete wavefield propagation of a phase-only object distribution $\mathbf{u}_0 = \exp(j\boldsymbol{\varphi}_0)$ and try to reconstruct this distribution from a given complex-valued observation in the sensor plane $\mathbf{u}_z = \mathbf{M} \circ \exp(j\boldsymbol{\varphi}_z)$, where $\circ$ stays for the Hadamard (elementwise) product, $\boldsymbol{\varphi}_0$ and $\boldsymbol{\varphi}_z$ are matrices of the phase distribution in the object and sensor planes, and $\mathbf{M}$ is an intensity (module) distribution in the sensor plane. We assume that $\boldsymbol{\varphi}_0 = \pi(\mathbf{u} - 1/2)$, where the matrix $0 \le \mathbf{u} \le 1$ is the square test-image (Baboon in our experiments) of the size $N_{y,0} = N_{x,0} = N_0 = 512$. The image in the sensor plane is square of the size $N_{y,z} = N_{x,z} = N_z = qN_0$, where the parameter $q \ge 1$ defines a redundancy of the sensor with respect to the object distribution. The pixels are square of the equal size in the sensor and object planes, $\Delta_{y,0} = \Delta_{x,0} = \Delta_0$, $\Delta_{y,z} = \Delta_{x,z} = \Delta_z$, $\Delta_z = \Delta_0 = 5$ μm. The accuracy criterion is the root mean square error (*RMSE*) calculated for the difference of the phase (angle) of the object distribution and its reconstruction (estimate).

4.1 Matrix ranks and reconstruction accuracy

Note, that while the matrices $\mathbf{A}_y$ and $\mathbf{A}_x$ are rectangular, $N_z \times N_0$, the matrices $\mathbf{A}_y^H\mathbf{A}_y$ and $\mathbf{A}_x^H\mathbf{A}_x$ are square, $N_0 \times N_0$, for any $N_z = qN_0$. The ranks of the matrices $\mathbf{A}_y^H\mathbf{A}_y$ and $\mathbf{A}_x^H\mathbf{A}_x$ depend on the sensor and

pixel sizes, distance between the sensor and object planes and on the parameter q. It is shown in [2] that the distance corresponding to the sampling conditions which appear in the discrete Fresnel transform enables the maximum value of the ranks of $\mathbf{A}_y^H \mathbf{A}_y$ and $\mathbf{A}_x^H \mathbf{A}_x$ and the object distribution reconstruction to be perfect or nearly perfect. We call this distance as the *"in-focus"* distance with notation $d_f|_q$. It is calculated as

$$d_f|_q = N_z \cdot \Delta_z \cdot \Delta_0 / \lambda = q \cdot N_0 \cdot \Delta_z \cdot \Delta_0 / \lambda \,. \tag{7}$$

In our experiments we assume that the pixels have a fixed size, while the distance d and the sensor redundancy parameter q are varying.

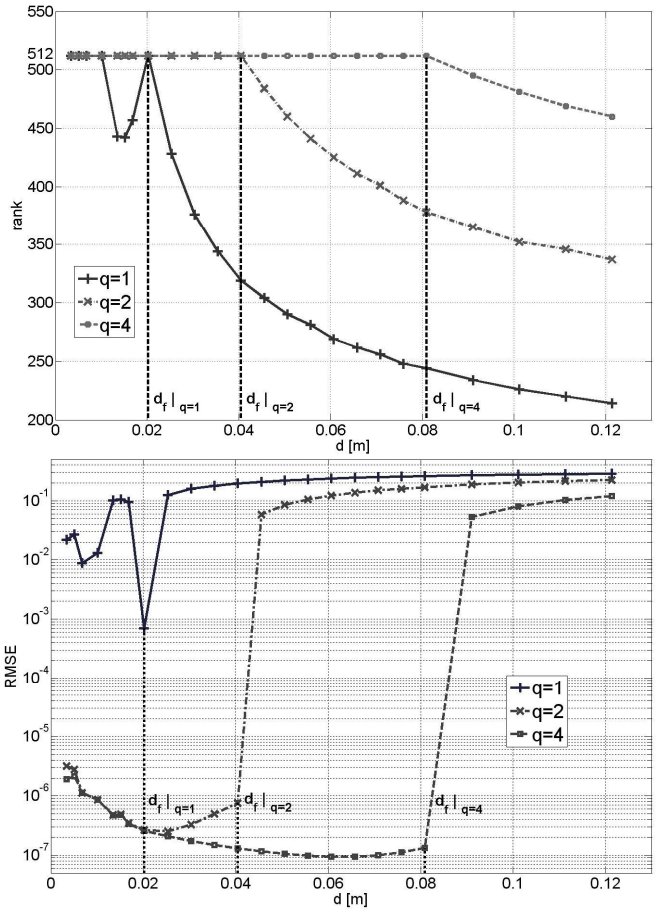

Fig. 1. The rank of $\mathbf{A}_y^H \mathbf{A}_y$ (top) and *RMSE* (bottom) versus the distance d for q= *{1, 2, 4}*

The numerical rank of the matrix $\mathbf{A}_y^H \mathbf{A}_y$ and the corresponding *RMSE* accuracy (in radian) of the phase-object distribution reconstruction are shown in Fig. 1 (top) and Fig. 1 (bottom) respectively for three different values of *q={1, 2, 4}*. These are complementary images allowing to track the dependence of the accuracy on the distance and to link this accuracy with the rank of the matrix. It is clear that the rank value close to the maximum value 512 results in a very high accuracy. For the redundant sensors of the size larger than the size of the object with *q=2* and *q=4* the ranks are decreasing functions for $d > d_f|_{q=2}$ and $d > d_f|_{q=4}$, respectively. These rank values are much higher than it is for *q=1*. We can see that if *q=2* or *q=4* we obtain the maximum values of the rank and practically perfect reconstruction for all $d \le d_f|_{q=2}$ or $d \le d_f|_{q=4}$, respectively. As soon as $d > d_f|_q$ the numerical ranks decreases and the accuracy of reconstruction is going down. For *q=1* the accuracy is uniformly worse than that is for *q={2, 4}*. Referring to the results shown in [2], we note that a very similar behavior is observed for the reconstruction accuracy of amplitude-object distributions.

4.2 Comparative accuracy analysis

The comparative accuracy analysis of the different algorithms for various distances *d* can be produced from the results shown in Fig. 2.

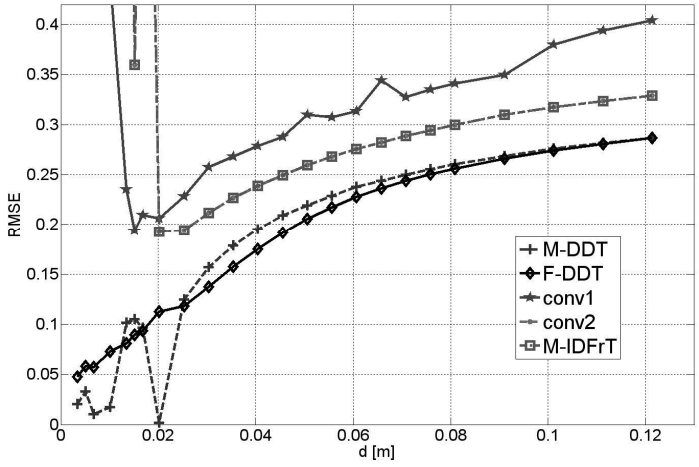

Fig. 2. The accuracy of the image restoration (*RMSE*) versus the distance *d* for the following algorithms: *M-DDT*, the recursive regularized inverse *F-DDT* [3], the convolutional inverse *conv1* and *conv2*, and *M-IDFrT* [2], $d_f|_{q=1}$ = 0.02 m

The regularized inverse *M-DDT* algorithm (see Eq. (6)) demonstrates the high-accuracy performance for nearly all distances. A quite close performance with sometimes slightly better results is shown by the recursive (10 iterations) regularized inverse frequency domain *F-DDT* [3]. It is emphasized that *M-DDT* enables the perfect reconstruction for $z = d_f|_q$. If the square pixels are of the equal size in the object and sensor planes and the corresponding images are of the equal size the standard double-size zero-padding convolutional algorithm (*conv2*) and matrix inverse discrete Fresnel transform (*M-IDFrT*) give practically identical results within the calculation accuracy. The curves corresponding to these algorithms are overlapping in Fig. 2. The accuracy of these algorithms is much better than it can be obtained by the ordinary convolutional algorithm (*conv1*).

Let the pixels be rectangular ($\Delta_{y,0} = \Delta_{y,z} = 8$ μm, $\Delta_{x,0} = \Delta_{x,z} = 5$ μm) and the same in the object and sensor planes. According to Eq. 2 and Eq. 3 the matrices $\mathbf{A}_y$ and $\mathbf{A}_x$ are different. In this case the calculation of the averaged matrices $\mathbf{A}_y$ and $\mathbf{A}_x$ and the choice of the in-focus distance become much more complex. The in-focus distance for *M-DDT* is calculated according to the following formulas [2]: $d = \min(d|_{f,y}, d|_{f,x})$, $d|_{f,y} = q \cdot N_{y,0} \cdot \Delta_{y,z} \cdot \Delta_{y,0} / \lambda = 0.05$ m, $d|_{f,x} = q \cdot N_{x,0} \cdot \Delta_{x,z} \cdot \Delta_{x,0} / \lambda = 0.02$ m.

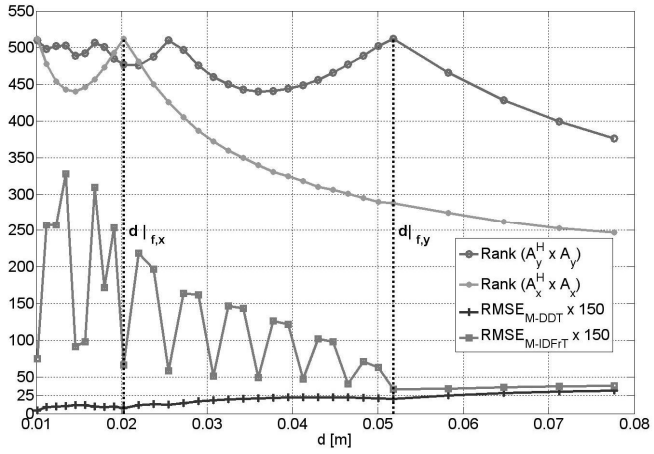

Fig. 3. The ranks of the matrices $\mathbf{A}_y^H \mathbf{A}_y$ and $\mathbf{A}_x^H \mathbf{A}_x$ for the rectangular pixels and *RMSE* for the wavefield reconstruction with the *M-DDT* and *M-IDFrT* algorithms versus the distance *d*

The numerical ranks of matrices $\mathbf{A}_y^H \mathbf{A}_y$ and $\mathbf{A}_x^H \mathbf{A}_x$ and the corresponding RMSE values versus the distance *d* are shown in Fig. 3. The best accuracy is obtained when the ranks of $\mathbf{A}_y^H \mathbf{A}_y$ and $\mathbf{A}_x^H \mathbf{A}_x$ are simultaneously close to their maximum values. For the considered parameters it happens at the in-focus distance equal to $d|_{f,x}$.

5 Conclusion

This paper concerns a novel discrete modeling for forward and backward propagation. The regularized inverse of the M-DDT is used for reconstruction of the object wavefield distribution. It is shown that the ranks of the used matrices serve as quite accurate predictors for the reconstruction accuracy. These sort of results have been demonstrated in [2] for the amplitude-modulation of the object distribution. It is done for the phase-modulation in this paper. Together these two papers prove that the ranks of the matrices of M-DDT can be used for design and optimization of experiments involving the wavefield reconstruction.

6 Acknowledgments

This research is supported by the Academy of Finland, project No. 213462 (Finnish Centre of Excellence program 2006 - 2011), and the work of Artem Migukin is funded by the Tampere Graduate School in Information Science and Engineering (TISE).

References

1. Kreis, Th. (2005) Handbook of Holographic Interferometry (Optical and Digital Methods). Wiley-VCH Gmbh&Co.KGaA, Weinheim.
2. Katkovnik, V, Migukin, A, Astola, J (2009) Backward discrete wavefield propagation modeling as an inverse problem: toward perfect reconstruction of wavefield distributions. Appl. Opt, 2009, http://www.cs.tut.fi/~lasip.
3. Katkovnik, V, Astola, J, Egiazarian, K (2008) Discrete diffraction transform for propagation, reconstruction, and design of wavefield distributions. Appl. Opt. 47, 3481-3493.